CHAPTER 3

RESULTS AND DISCUSION

Chromium (VI) in wastewater was removed by using iron oxide – coated sand (IOCS) and chromium in the filtrate was determined by graphite furnace atomic absorption spectrometer (GFAAS). Several analysis conditions for determination of chromium (VI) by graphite furnace atomic absorption spectrometer were optimized to obtain the best peak performance.

3.1 Optimization of graphite furnace atomic absorption spectrometer (GFAAS)

3.1.1 Pyrolysis Temperature

The purpose of the analysis step is to volatilize inorganic and organic matrix components selectively from samples, leaving the analyte element in a less complex matrix for analysis. During this step, the temperature was increased as high as possible to volatilize matrix components but below the temperature at which analyte loss would occur. The temperature selected for the pyrolysis step will depend on the analyte and the matrix. The pyrolysis temperature was studied in experiment 2.3.5.1. Table 3-1 and Figure 3-1 were the results of the pyrolysis temperature.

Table 3-1 The absorbance of the pyrolysis temperature at 30 µg L^{-1} Cr (VI), 20 µL

Pyrolysis temperature (^{o}C)	Absorbance ± SD*
1100	0.1486 ± 0.0068
1200	0.1488 ± 0.0061
1300	0.1489 ± 0.0047
1400	0.1477 ± 0.0055
1500	0.1483 ± 0.0023
1600	0.1456 ± 0.0026
1650	0.1453 ± 0.0078
1700	0.1366 ± 0.0045
1800	0.0804 ± 0.0064

*3 replications, RSD < 4%

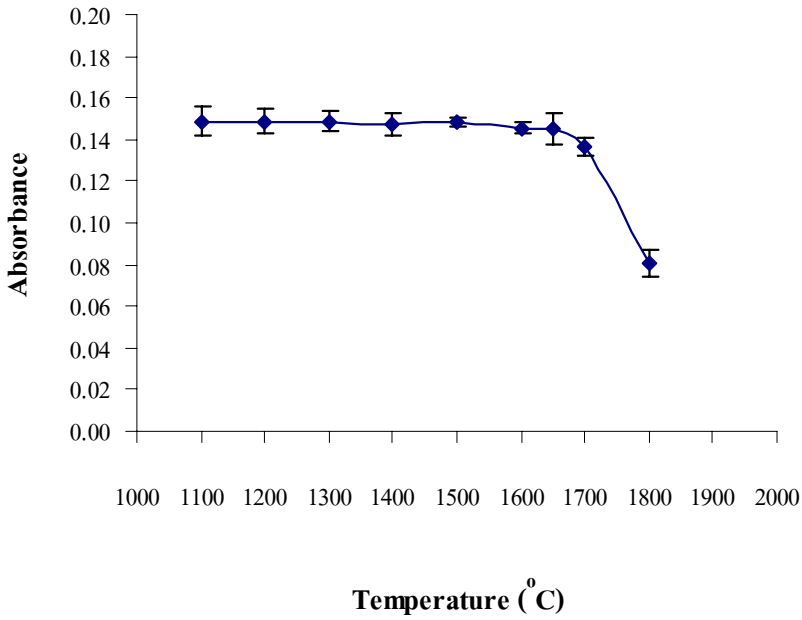

Figure 3-1 The relationship between absorbance of 30 µg L^{-1} Cr (VI) standard working solution and the pyrolysis temperature (^{o}C)

During this step, the temperature was increased as high as possible to volatilize matrix components but below the temperature at which analyte loss would occur. The optimum pyrolysis temperature was 1500 ^{o}C.

3.1.2 Atomization temperature

The purpose of the atomization step is to produce an atomic vapor of the analyte elements, thereby allowing atomic absorption to be measured. The temperature in this step was increased to the point where the dissociation of volatilized molecular species occurs. The atomization temperature was studied in experiment 2.3.5.2. The absorbance of atomization temperature is shown in Table 3-2 and Figure 3-2.

Table 3-2 The effect of the atomization temperature on the absorbance of 30 µg L^{-1} Cr (VI), 20 µL

Atomization temperature (^{o}C)	Absorbance ± SD *
1800	0.0216 ± 0.0050
1900	0.0587 ± 0.0185
2000	0.1045 ± 0.0142
2100	0.1666 ± 0.0004
2200	0.1771 ± 0.0010
2300	0.1721 ± 0.0013
2400	0.1655 ± 0.0018

* 3 replications, RSD < 4%

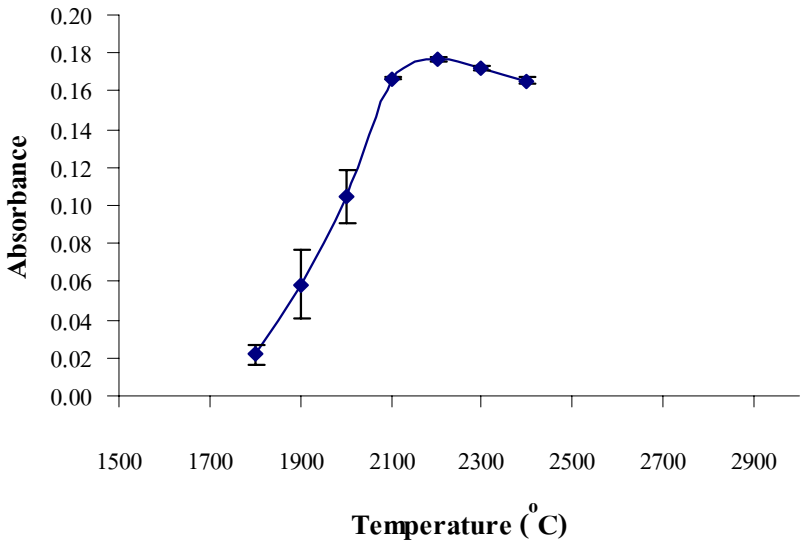

Figure 3-2 The relationship between absorbance of 30 µgL^{-1} Cr (VI) standard working solution and the atomization temperature (^{o}C)

The optimum atomization temperature should be a point where maximum absorbance occurs with minimum temperature, which is 2200 ^{o}C. However, the absorbance profile at this temperature showed a broad and tailing peak, while the profile at 2300 ^{o}C showed a well defined peak (Figure 3-3). Thus we choose the optimum atomization temperature at 2300 ^{o}C.

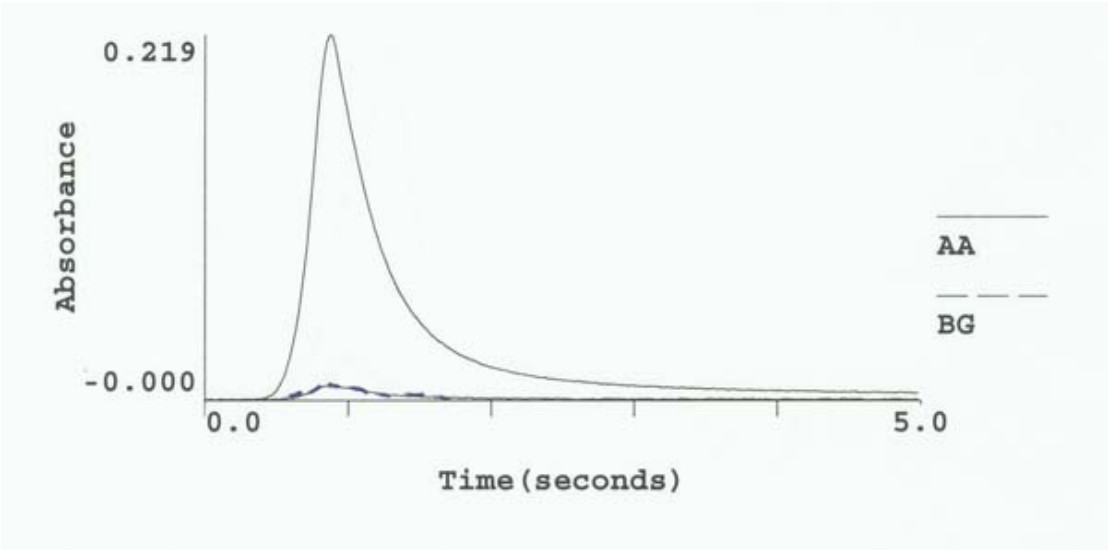

Figure 3-3 Peak shape of 30 µg L^{-1} Cr (VI) standard working solution at optimum temperature

3.1.3 Detection limit (DL)

The detection limit (DL) is defined as the smallest concentration that can be reported as being present in a sample with a specified level of confidence.

Most commonly, the detection limit is defined operationally as the analyte concentration yielding an analytical signal equal to some confidence factor *k* time the SD of the blank measurement (s_{bk}) or the concentration where $S = ks_{bk}$, Alternatively, it can be defined as the analyte concentration where $S/N = k$, which is equivalent to the first definition if $N = s_{bk}$, so $S/N = ks_{bk}/s_{bk} = k$. The DL can also be directly calculated from

$$DL = ks_{bk} / m$$

Here a linear calibration curve near the DL with calibration slope *m* is assumed, so $S = mc$ or $c = S/m$ and $S = ks_{bk}$. The factor *k* is most often chosen to be 2 or 3 (Ingle and Crouch, 1988).

The absorbance of blanks were carried out for evaluating detection limit of Cr (VI). The results are shown in Table 3-3 and Figure 3-4.

Table 3-3 The data of the blank measurements of Cr (VI), n = 10

Replicate	Absorbance of blank for Cr(VI), n=10
1	0.0009
2	0.0006
3	0.0005
4	-0.0002
5	0.0001
6	0.0000
7	-0.0001
8	0.0001
9	0.0002
10	0.0023
	Mean = 0.0004 SD = 0.0007

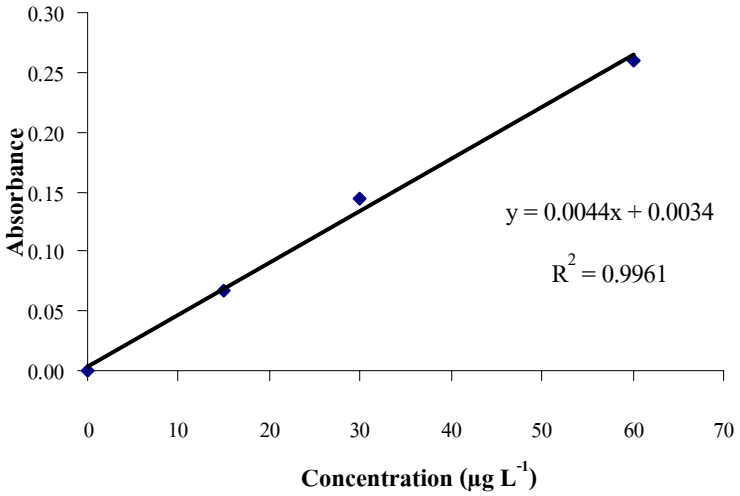

Figure 3-4 The calibration curve of Cr (VI)

The detection limit for Cr (VI) standard solution with optimum conditions of GFAAS.

$$DL = kS_{bk} / m$$

$$= 3S_{bk}/m;\ S_{bk} = 0.0007\ ,\ m = 0.0044$$

$$DL = 0.48\ \mu g\ L^{-1}$$

3.1.4 Linear dynamic range (Linearity)

The linear dynamic range of Cr (VI) was investigated by experiment 2.3.5.4 and the absorbance of various concentrations of standard Cr (VI) was obtained in Table 3-4 and Figure 3-5. Three replications were done for each concentration and the results showed high precision with all relative standard deviations (RSD) lower than 4%. The system provided a wide linear dynamic range from 1-100 µg L^{-1} with a very good correlation coefficient, $R^2 > 0.99$.

Table 3-4 The relationship between the peak area and the various Cr (VI) standard concentration (µg L^{-1})

Concentration(µg L^{-1})	Absorbance ± SD*
1.0	0.0078 ± 0.0023
5.0	0.0306 ± 0.0004
10.0	0.0582 ± 0.0024
25.0	0.1387 ± 0.0041
50.0	0.2713 ± 0.0038
100.0	0.5025 ± 0.0068
150.0	0.6622 ± 0.0110
200.0	0.8099 ± 0.0061
225.0	0.8661± 0.0069
250.0	0.9332 ± 0.0026
270.0	0.9836 ± 0.0081
300.0	1.0445 ± 0.0113

* 3 replications, RSD < 4%

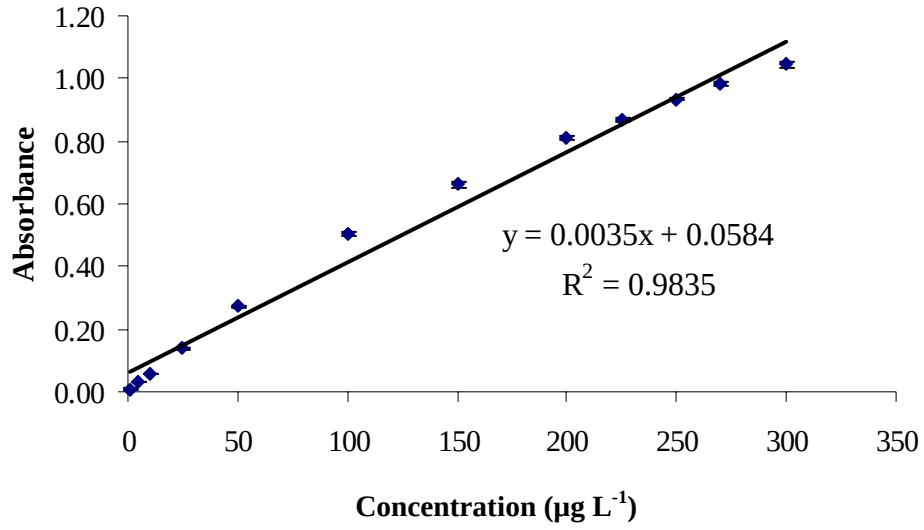

Figure 3-5 The linear dynamic range of Cr (VI) standard concentration at 1-300 µg L^{-1}

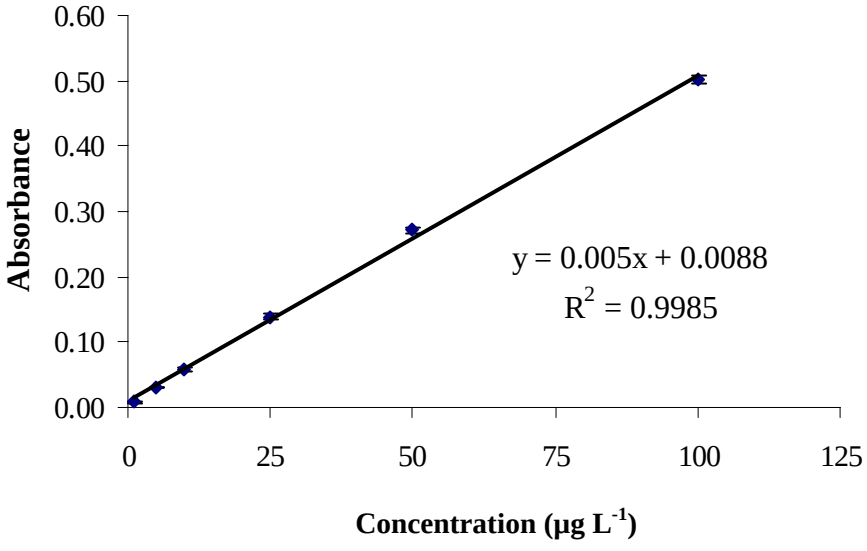

Figure 3-6 The linear dynamic range of Cr (VI) standard concentration at 1-100 µg L^{-1}

3.1.5 Accuracy and precision

The accuracy of this technique was evaluated from the percent recovery as mentioned in section 2.3.5.5 and the result is shown in Table 3-5.

Table 3-5 The percent recovery of Cr (VI) at concentration of 30.0 μg L^{-1}.

Metals	Added Amount (μg L^{-1})	Found Amount (μg L^{-1})	% Recovery	%RSD
Cr(VI)	30.0	31.4	104.67	2.55

∗ 3 replications, RSD < 10 %

From this results, it can be concluded that the percentage recovery of Cr (VI) 30.0 μg L^{-1} was 104.67 in agreement with EPA method 7010 (85-115 %).

In addition, the precision of this method was also evaluated as % RSD. The % RSD of Cr (VI) was obtained from this method was 2.55 in good agreement with from EPA method (< 10 %).

3.2 Chromium (VI) removal by using iron oxide-coated sand (IOCS)

3.2.1 Effect of sand size on removal Cr(VI) by IOCS

If the diameter of sand is different, the percentage of removal Cr (VI) by IOCS is different. From experiment 2.4.3. Size of sand was investigated by varying at 0.330-0.425 (mesh size 50-40), 0.425-0.600 (mesh size 40-30) and 0.600-0.850 mm (mesh size 30-20). The results of this condition are shown in Table 3-6, Figure 3-7.

Table 3-6 Summarises the percentage removal of 10 mg L^{-1} Cr (VI) by IOCS at the different sizes of sand

Size of sand (mm)	% Removal of Cr (VI) ± SD*
0.330-0.425	97.7 ± 3.81
0.425-0.600	93.3 ± 2.33
0.600-0.850	89.2 ± 7.05

* 3 replicates, RSD < 10 %

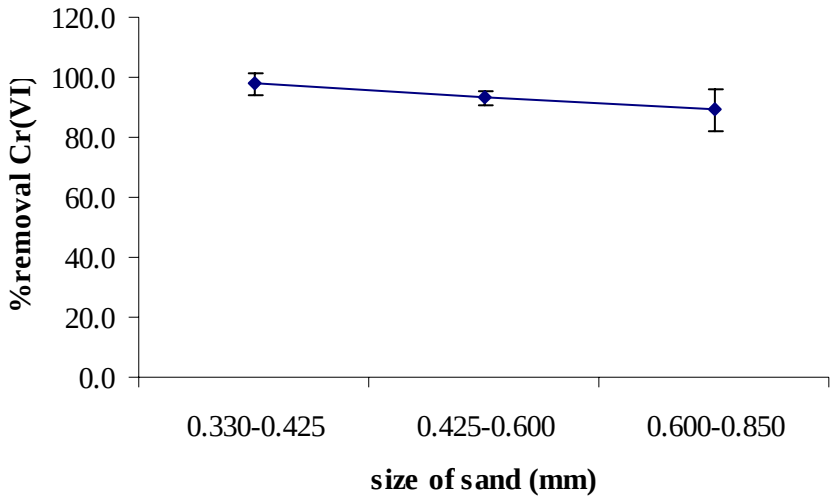

Figure 3-7 The relationship between size of sand and the percentage of removal 10 mg L^{-1} Cr (VI) by IOCS

From this experiment, the results show that the removal of Cr (VI) by IOCS increases with the decreases size of sand. Maximum removal Cr (VI) 97.7% was achieved at size of sand 0.330-0.425 mm (mesh size 50-40).

Consequently, this size of sand was selected for the removal Cr (VI) by IOCS of the experiment.

3.2.2 Comparison between uncoated and $FeCl_3$ coated sand

The removal Cr (VI) by uncoated and $FeCl_3$ coated sand are shown in Table 3-7 and Figure 3-8.

Table 3-7 The percentage removal of 10 mg L^{-1} Cr (VI) by uncoated and $FeCl_3$ coated sand

Conditions	% Removal of Cr (VI) ± SD*
$FeCl_3$ coated sand	100.3 ± 0.70
$FeCl_3$ uncoated sand	56.3 ± 1.90

*3 replications, RSD < 10%

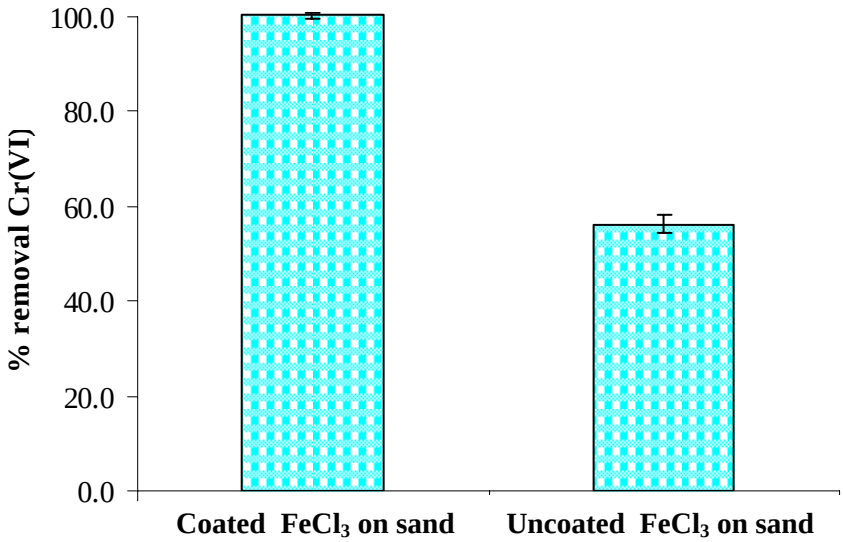

Figure 3-8 The percentage removal of 10 mg L^{-1} Cr (VI) by uncoated and $FeCl_3$ coated sand

It can be concluded from the results in Table 3-7 and Figure 3-8 that the $FeCl_3$ coated sand that gave higher a percentage removal Cr (VI) than $FeCl_3$ uncoated sand.

3.2.3 Effect of pH on removal Cr(VI) by IOCS

From experimental 2.4.5, it was investigated pH of solution before passing the column, by varying pH at 3,5,7,8 and 9. The removal Cr (VI) by IOCS using different pH, the results are shown in Table 3-8 and Figure 3-9.

Table 3-8 The percentage removal of 10 mg L^{-1} Cr (VI) by IOCS at different pHs

pH	% Removal of Cr (VI) ± SD*
3	92.8 ± 2.78
5	97.5 ± 2.11
7	100.3 ± 0.76
8	95.6 ± 3.03
9	96.1 ± 1.88

*3 replications, RSD < 10%

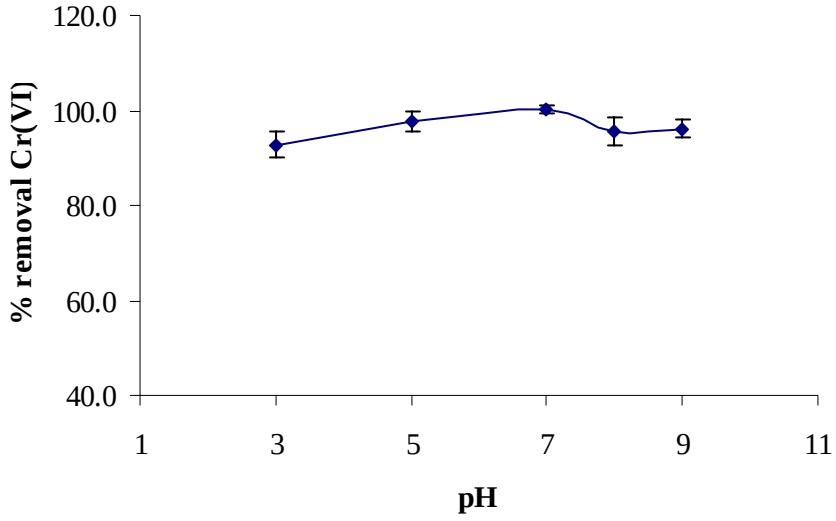

Figure 3-9 The relationship between pH of solution and the percentage of removal 10 mg L^{-1} Cr (VI) by IOCS

From the result in Table 3-8 and Figure 3-9, the effect of pH on removal of 10 mg L^{-1} Cr (VI) by IOCS is shown. The removal increased as pH increased and the removal decreased occurred above pH 8. A 100 % Removal of of Cr (VI) observed at pH 7. $HCrO_4^-$ is predominant below pH 7. Therefore $HCrO_4^-$ participated in coprecipitation with iron(III) hydroxide (Aoki and Munemori, 1982).

3.2.4 Effect of concentration of $FeCl_3$ on removal Cr (VI) by IOCS

From experiment 2.4.6, the concentration of $FeCl_3$ was investigated by varying at 0.25, 0.50, 0.70, 0.90 and 1.00 M. The removal Cr (VI) by IOCS using different concentration of $FeCl_3$, the results are shown in Table 3-9 and Figure 3-10.

Table 3-9 The percentage removal of 10 mg L^{-1} Cr (VI) by IOCS at different concentrations of $FeCl_3$

Concentration of $FeCl_3$ (M)	% Removal of Cr (VI) ± SD*
0.25	90.0 ± 2.01
0.50	92.0 ± 4.47
0.70	93.0 ± 3.15
0.90	93.1 ± 4.62
1.00	100.5 ± 0.70

*3 replications, RSD < 10%

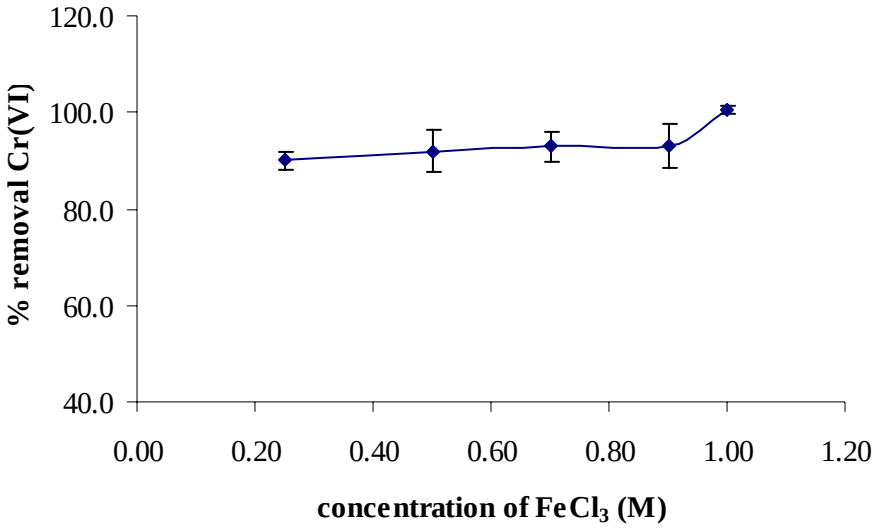

Figure 3-10 The relationship between concentration of $FeCl_3$ and the percentage of removal 10 mg L^{-1} Cr (VI) by IOCS

From this experiment, the results in Table 3-9 and Figure 3-10, show that the effect of concentration of $FeCl_3$ on removal 10 mgL^{-1} Cr (VI) by IOCS. The removal increased as the concentration of $FeCl_3$ increased. Maximum removal Cr (VI) 100 % is achieved at 1.00 M $FeCl_3$. This concentration of $FeCl_3$ gave the concentration of Cr (VI) less than acceptable level (Notification the Ministry of Science, Technology and Environment, 1992). So we selected 1.00 M $FeCl_3$ for the experiment.

3.2.5 Effect of flow rate through IOCS on removal Cr (VI) by IOCS

From experiment 2.4.7. The flow rate was varied from 1.0 – 7.5 mL min^{-1} and the results are shown in Table 3-10 and Figure 3-11.

Table 3-10 The percentage removal of 10 mg L^{-1} Cr (VI) by IOCS at various flow rate**s**

Flow rate ($mLmin^{-1}$)	% Removal of Cr (VI) ± SD*	Residence time (min)
1.0	91.3 ± 0.70	13
2.5	86.9 ± 1.22	5
5.0	86.0 ± 3.85	3
7.5	87.2 ± 3.10	2

*3 replications, RSD < 10%

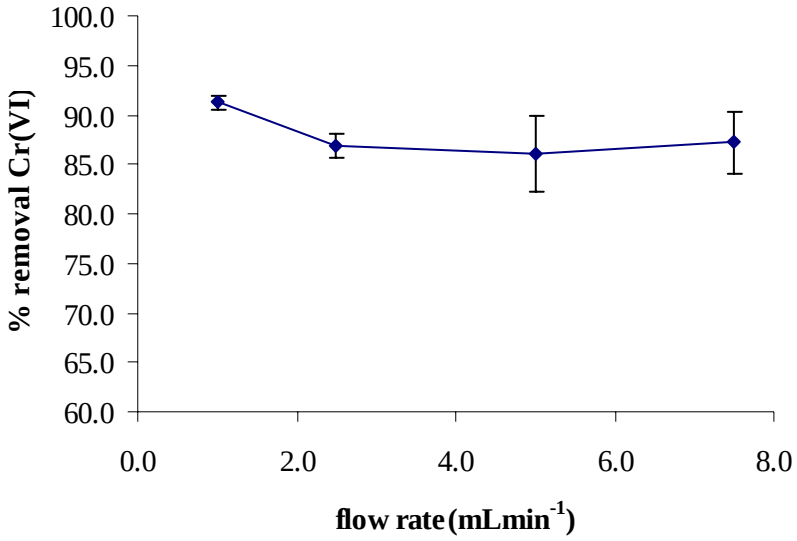

Figure 3-11 The relationship between flow rate and the percentage of removal 10 mg L^{-1} Cr (VI) by IOCS

From the results obtained in Table 3-10 and Figure 3-11, it was found that increase in flow rate causes a decrease in removal efficiency. The decrease in removal efficiency with the increase in flow rate indicates the adsorption of heavy metals on sand. A reduction of adsorption capacity is expected at higher flow rate (Muhammad *et al*, 1997). The flow rate at 1.0 mL min^{-1} gave maximum removal.

3.2.6 Effect of time for coating $FeCl_3$ on sand on removal Cr(VI) by IOCS

The time for coating $FeCl_3$ on sand was varied as in 2.4.8 and the results are shown in Table 3-11 and Figure 3-12.

Table 3-11 The percentage removal of 10 mg L^{-1} Cr (VI) by IOCS at various times for coating $FeCl_3$ on sand

Time for coating $FeCl_3$ on sand (hour)	% Removal of Cr (VI) ± SD*
1.0	91.3 ± 1.82
3.0	92.3 ± 1.04
5.0	94.2 ± 1.68
7.0	93.4 ± 1.34
9.0	94.1 ± 1.01
12.0	91.4 ± 0.35

*3 replications, RSD < 10%

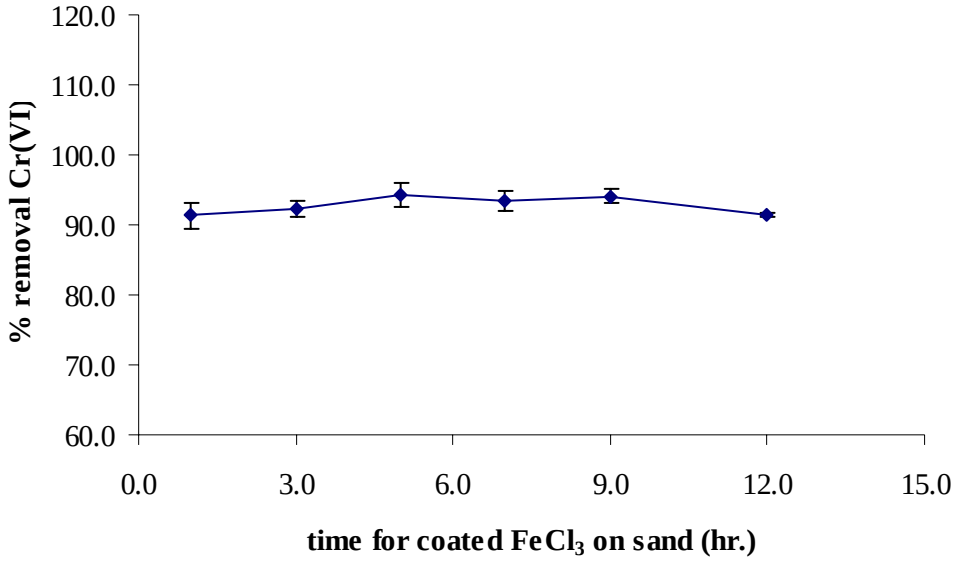

Figure 3-12 The relationship between times for coating $FeCl_3$ on sand and the percentage of removal 10 mg L^{-1} Cr (VI) by IOCS

It can be concluded from the results in Table 3-11 and Figure 3-12 that the maximum removal of chromium was found when the sand was coated for 5.0 h. In order to shorten the time consuming in chromium removal, the statistic t-test of this data set was performed. It was found that no significant different in 1.0 h and 5.0 h. Thus we chose 1.0 h for coating $FeCl_3$ on sand.

3.2.7 Effect of weight of sand on removal Cr(VI) by IOCS

From experiment 2.4.9. The weight of sand was varied from 10 – 30 grams and the results are shown in Table 3-12 and Figure 3-13.

Table 3-12 The percentage removal of 10 mg L^{-1} Cr (VI) by IOCS at various weights of sand

Weight of sand (g)	% Removal of Cr (VI) ± SD*
10	58.8 ± 2.58
20	90.9 ± 0.96
30	99.7 ± 0.19

*3 replications, RSD < 10%

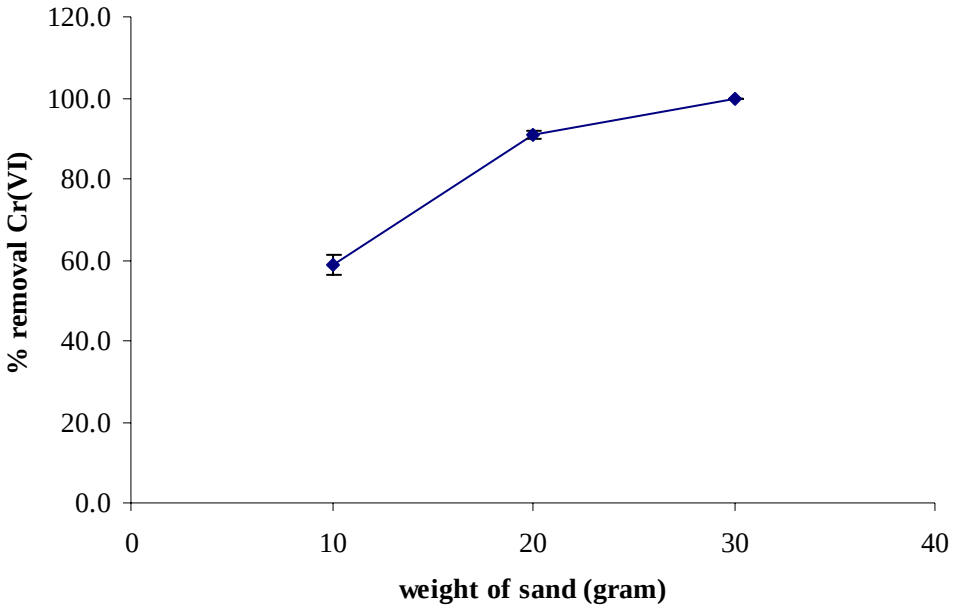

Figure 3-13 The relationship between weight of sand and the percentage of removal 10 mg L^{-1} Cr (VI) by IOCS

It can be concluded from the results in Table 3-12 and Figure 3-13 that the removal efficiency increases with the increase of the weight of sand. The removal efficiency increases sharply with the weight of sand and optimum removal is achieved at 30 g. As depth (weight of sand) increases, the total adsorption capacity also increases. Adsorption is one of the likely mechanism for the removing heavy metal by SSF (SSF = Slow Sand Filtration) (Muhammad *et al.*, 1997).

3.2.8 Effect of anion on removal Cr (VI) by IOCS

From experiment 2.4.10. Effect of anion on removal Cr (VI) by IOCS was investigated by varying type of anion at 500 mg L^{-1} of NO_3^-, 500 mg L^{-1} of SO_4^{2-} and 500 mg L^{-1} of PO_4^{3-}, respectively and the results are shown in Table 3-13 and Figure 3-114.

Table 3-13 The percentage removal of 10 mg L^{-1} Cr (VI) by IOCS at various types of anion

Type of anion	% Removal of Cr (VI) ± SD*
NO_3^-	99.9 ± 0.09
SO_4^{2-}	99.1 ± 0.34
PO_4^{3-}	99.0 ± 0.18

*3 replications, RSD < 10%

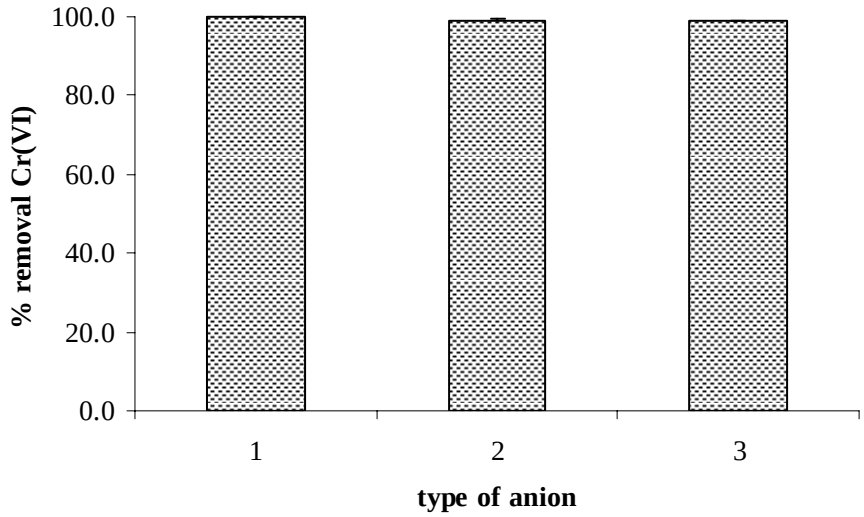

Figure 3-14 The relationship between type of anion and the percentage of removal 10 mg L^{-1} Cr (VI) by IOCS, 1 = NO_3^-, 2 = SO_4^{2-}, 3 = PO_4^{3-}

It can be suggested from the results in Table 3-13 and Figure 3-14 that the affinity of $HCrO_4^-$ / CrO_4^- for iron oxide coated sand was much stronger than NO_3^- SO_4^{2-} and PO_4^{3-}.

3.2.9 The comparison between the calibration and standard addition method for determination of Cr (VI) spiked in wastewater samples

This experiment was performed to compare standard method between calibration and standard addition for determination Cr (VI) spiked in wastewater samples after removal Cr (VI) by IOCS. The results are shown in Table 3-14 and Figure 3-15.

Table 3-14 The comparison of peak area between calibration and standard addition method for determination of Cr (VI) spiked in wastewater

Conc. (μg L^{-1})	Calibration curve (± SD)*	Standard addition (± SD)*
0.0	0.0000 ± 0.0057	0.0169 ± 0.0032
15.0	0.1557 ± 0.0044	0.1735 ± 0.0019
30.0	0.3136 ± 0.0010	0.3275 ± 0.0072
60.0	0.6341 ± 0.0005	0.6829 ± 0.0025

* 3 replications, RSD< 10 %

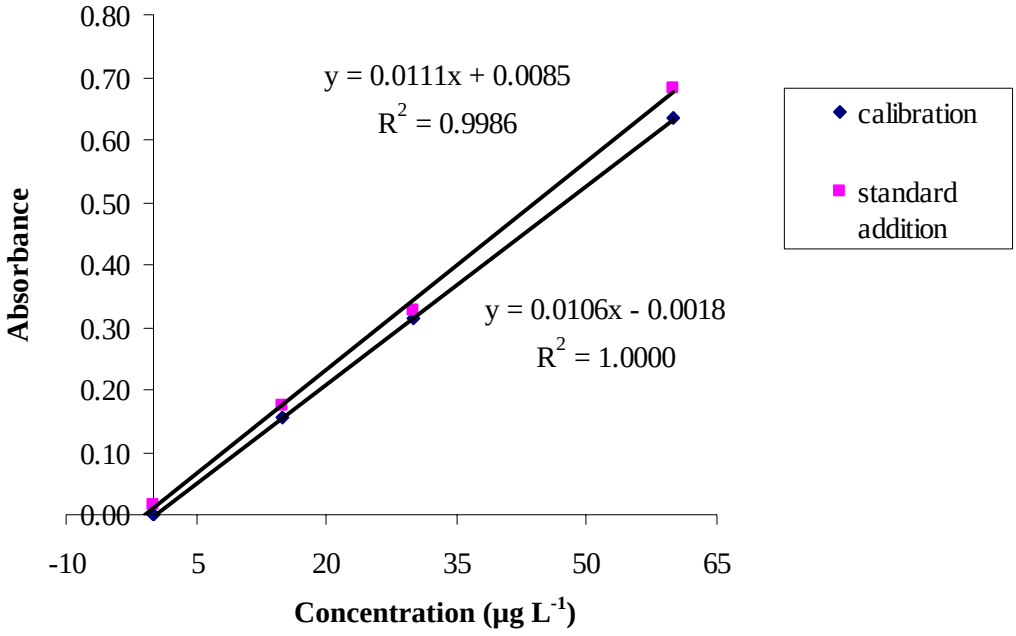

Figure 3-15 The comparison of calibration curve and standard addition for Cr (VI) determination in wastewater

From the Table 3-14 and Figure 3-15, it was found that the slope of Cr (VI) when compare calibration and standard addition method do not parallel. It can be concluded that there is a matrix interference occur in wastewater samples. Therefore, Cr (VI) concentration was calculated by using a standard addition method for Cr (VI) determination in wastewater samples.

3.2.10 Removal of Cr (VI) spiked in wastewater samples by IOCS

Four samples of wastewater were collected in feedmill manufactory located in Banpru sub-district, Hat Yai city municipality, Songkhla province. Cr (VI) spiked in wastewater samples were removed Cr (VI) by IOCS and analyzed by GFAAS at optimum conditions. The results are shown in Table 3-15.

Table 3-15 The percentage of removal Cr (VI) in four Cr (VI) spiked in wastewater samples

Locations	% Removal of Cr (VI) ± SD*
Facultative pond	97.5 ± 0.03
Final polishing pond 1	98.5 ± 0.08
Final polishing pond 2	98.1 ± 0.05
Constructed wetland	99.1 ± 0.04

* 3 replications

From the Table 3-15, the results shown that the percentage of removal Cr (VI) in four wastewater samples is in the range from 97.5 – 99.1 %. The residue concentration of Cr (VI) spiked in wastewater samples after removal by IOCS is in the range from 0.09 mg L^{-1} – 0.25 mg L^{-1}, agree with chromium concentration in industries effluent standards (not more than 0.25 mg L^{-1}) (Notification the Ministry of Science, Technology and Environment, 1992).